Journal of Marine Research, 43, 83–111, 1985

Average velocity and transport of the Gulf Stream near 55W

by P. L. Richardson[1]

ABSTRACT

Long-term current measurements made with surface drifters, SOFAR floats at 700 m and 2000 m, and current meters at 4000 m have been combined to produce for the first time a vertical section of directly measured average zonal currents in and adjacent to the Gulf Stream. The results from the different data sets are remarkably consistent in showing three vertically coherent zonal jets—the Gulf Stream and two flanking countercurrents. The consistency in location, velocity and transport (per unit width) of these currents supports the conclusion that these are real features of the long-term average velocity field. The current jets coincide with a region of high eddy kinetic energy and its gradient, implying a dynamical connection.

The Gulf Stream is defined to be the eastward current bounded by the countercurrents. The surface Stream is ~900 km wide and has a maximum eastward velocity of 28 cm s^{-1} at 39.5N, averaged over a one degree latitude band. The Stream extends to the sea floor about 200 km south of its surface axis. The deep Stream is only ~200 km wide and has a maximum mean velocity of 7 cm s^{-1}. The total mean volume transport of the Stream is estimated to be 93 × 10^6 m^3 s^{-1} by fitting a smooth transport profile to the four directly measured values. About a third of this is depth-independent. Including estimates of local wind-driven surface velocity diminishes the total transport by 8 × 10^6 m^3 s^{-1}, to 85 × 10^6 m^3 s^{-1}. The mean transport is significantly less than the estimated synoptic transport of the Stream in this region, approximately 150 × 10^6 m^3 s^{-1}.

The subsurface Stream is flanked by relatively narrow, westward flowing countercurrents. The combined westward transport of the countercurrents is more than enough to locally recirculate the increase of Gulf Stream transport over the 30 × 10^6 m^3 s^{-1} wind-driven component of the subtropical gyre, returned in a gyre scale flow. The northern countercurrent, located between the Stream and continental shelf and rise, transports 41 × 10^6 m^3 s^{-1}. Part of this westward transport is the mean southwestward flow of the Western Boundary Undercurrent, which transports 10 to 15 × 10^6 m^3 s^{-1}. The southern countercurrent is located between 35–37N and transports about 29 × 10^6 m^3 s^{-1}. Part of this transport (~12 × 10^6 m^3 s^{-1}) is probably recirculated as eastward flow south of 35N. The net transport across 55W north of 35N is eastward and equal to 11–23 × 10^6 m^3 s^{-1} (the low value includes the wind correction).

1. Introduction

Despite the Gulf Stream's central importance to the general circulation of the North Atlantic, our knowledge of the Stream's mean velocity structure and transport downstream from Cape Hatteras has remained rudimentary. This is because of the difficulty of obtaining direct long-term measurements in such a swift and variable

1. Woods Hole Oceanographic Institution, Woods Hole, Massachusetts, 02543, U.S.A.

current. Existing moored current meter records in the Stream are confined to the deep region below the high speed currents (Luyten, 1977; Schmitz, 1977, 1978, 1980). Only within the last year has technology made it possible to successfully maintain long-term current meter moorings in the upper portion of the Stream (H. Bryden, R. Hendry, personal communications).

Recently, however, freely drifting buoys and SOFAR floats have been tracked in the Stream in sufficiently large numbers to make possible meaningful estimates of average velocity and transport. In this report, two years of float data at 700 m and 2000 m are combined with some earlier data from surface drifters and deep moored current meters to produce a vertical section of average zonal velocity through the Gulf Stream and a first direct measurement of its average transport in the deep North Atlantic.

2. Background

As it flows northeastward from the Straits of Florida and into the deep North Atlantic, the Gulf Stream increases in volume transport, from 30×10^6 m^3 s^{-1} at the Straits to a maximum of about 150×10^6 m^3 s^{-1} south of Nova Scotia (Knauss, 1969; Niiler and Richardson, 1973; Worthington, 1976). This increase is thought to be largely due to the instability of the Stream and the resulting energetic time-dependent eddy motions, which coincide with the region of maximum transport. Some eddy-resolving numerical models suggest that the eddies drive a deep eastward abyssal flow under the surface Stream and a largely barotropic recirculation on both sides of the Stream (Holland *et al.*, 1983). Recently, data from deep moored current meters along 55W have given us a first look at the structure of the deep mean Gulf Stream and its recirculation (Schmitz, 1977, 1978, 1980; see also Hogg, 1983). Unfortunately, these data do not tell us about the upper region of the Stream, nor are there other long-term measurements of the Stream's velocity and transport in the deep North Atlantic.

South of Cape Hatteras, where the Stream flows in relatively shallow water and seldom meanders far from shore, the mean transport of the Stream is well documented (Richardson *et al.*, 1969; Knauss, 1969; Niiler and Richardson, 1973). Downstream from Hatteras the Stream flows in water 5000 m deep, makes large amplitude meanders, and sheds intense current rings. The enormous time and space variability of the Stream in this region makes the measurement of transport very difficult.

Only six estimates of absolute Gulf Stream transport for the region 50–70W have been made.[2] Two methods were used. In the first, velocity sections were made across the Stream using transport floats—instruments that fall freely through the water and directly measure transport per unit width. Three repeated sections measured by Barrett and Schmitz (1971) gave transports of 165, 203, and 129×10^6 m^3 s^{-1}. The

2. Halkin and Rossby (1984) presented recent results of work in progress concerning the velocity and transport of the Stream near 73W. Repeated velocity sections across the Stream are being analyzed to resolve synoptic and time averaged transport.

mean of these is 166×10^6 m^3 s^{-1}. Each section was made within a few days and thus these values are representative of the synoptic transport.

The second method combines geostrophic (baroclinic) velocity sections with absolute velocity measured by deep floats or current meters. Five estimates using this technique are 147×10^6 m^3 s^{-1} (Fuglister, 1963), 101×10^6 m^3 s^{-1} (Warren and Volkmann, 1968), 130×10^6 m^3 s^{-1} (Clarke and Reiniger, 1973), 226×10^6 m^3 s^{-1} (Robinson *et al.*, 1974), 79×10^6 m^3 s^{-1} (Clarke *et al.*, 1980). Worthington (1976) charted the downstream variation in transport of the Stream and showed it to have a maximum transport of 150×10^6 m^3 s^{-1} south of Nova Scotia. He says (Worthington, 1976) that his maximum value was strongly biased in favor of Fuglister's (1963) value of 147×10^6 m^3 s^{-1} near 64W.

Both methods have the problem that it is very difficult to determine the limits or edges of the Stream. Velocity sections usually show a complicated pattern of meanders, multiple crossings of the Stream, eddies, countercurrents and small-scale embedded jets. These features frequently change from section to section, and it is not obvious which of them to include as Gulf Stream transport. Moored current meter measurements under and near the Stream reveal large amplitude, 50 cm/sec, time-dependent fluctuations of one month period typically (Luyten, 1977). It is an unsolved problem how to suitably combine these strongly fluctuating velocities with the more stable hydrographic and geostrophic features (Clarke *et al.*, 1980). Some of the early transport estimates (Fuglister, 1963) were based on a few very short (few days) velocity measurements sometimes not even overlapping in time with the hydrographic measurements. Using the deep float or current meter velocity tends to increase the transport over the geostrophic transport relative to the sea floor by large amounts. Fuglister (1963) reports an increase from 88×10^6 m^3 s^{-1} relative to zero velocity at the sea floor to 147×10^6 m^3 s^{-1} with float velocities. In an extreme case, Robinson *et al.* (1974) report transport of 77×10^6 m^3 s^{-1} relative to the sea floor and an absolute transport of 226×10^6 m^3 s^{-1}. These problems—determining the limits of the Stream and combining direct and geostrophic velocities—raise serious questions about the representativeness and accuracy of available transport estimates.

The inverse technique has been applied to hydrographic sections across the Stream (Wunsch, 1978). The resulting calculated transport of the Stream is strongly dependent on the initial chosen depth of zero velocity used. For example, calculated transport was 80×10^6 m^3 s^{-1} for 2000 m and 124×10^6 m^3 s^{-1} for the sea floor. Thus, this method has not been very helpful in refining our idea of the average Gulf Stream transport.

3. Data and methods

Twenty-five neutrally buoyant SOFAR floats were launched and tracked at several sites in and adjacent to the Gulf Stream along 55W and between 30–45N (Fig. 1). Floats were launched in pairs at depths of 700 m and 2000 m. Thirteen floats were launched in April 1980 and twelve in August 1981. Data from four additional floats

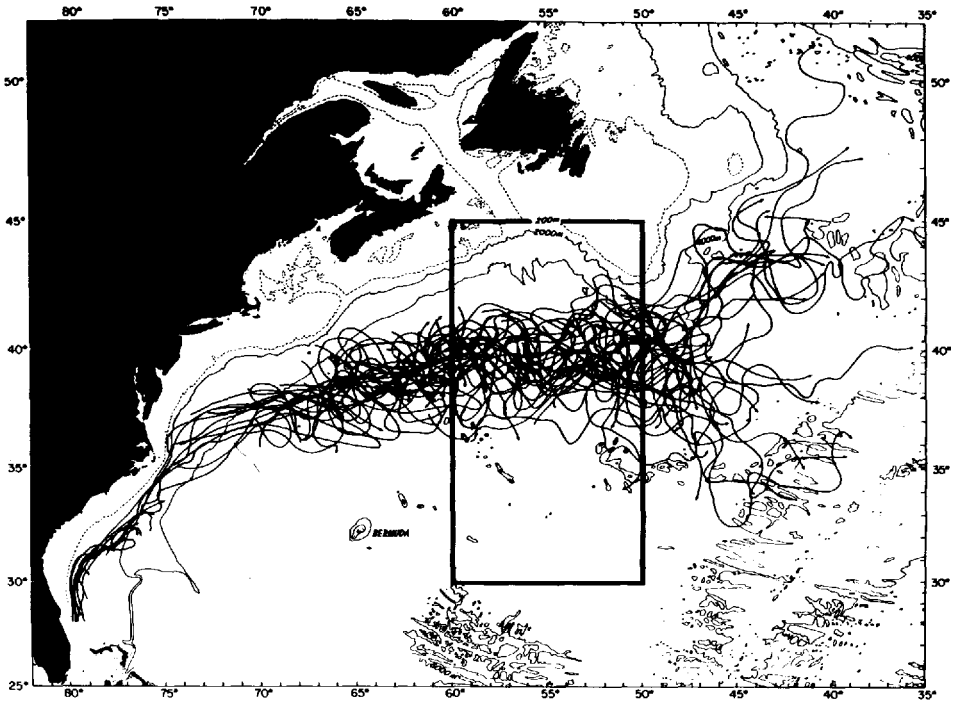

Figure 1a. Location of the study region, 30–45N, 50–60W. Trajectories of surface drifters in the Gulf Stream show its paths (from Richardson, 1983b).

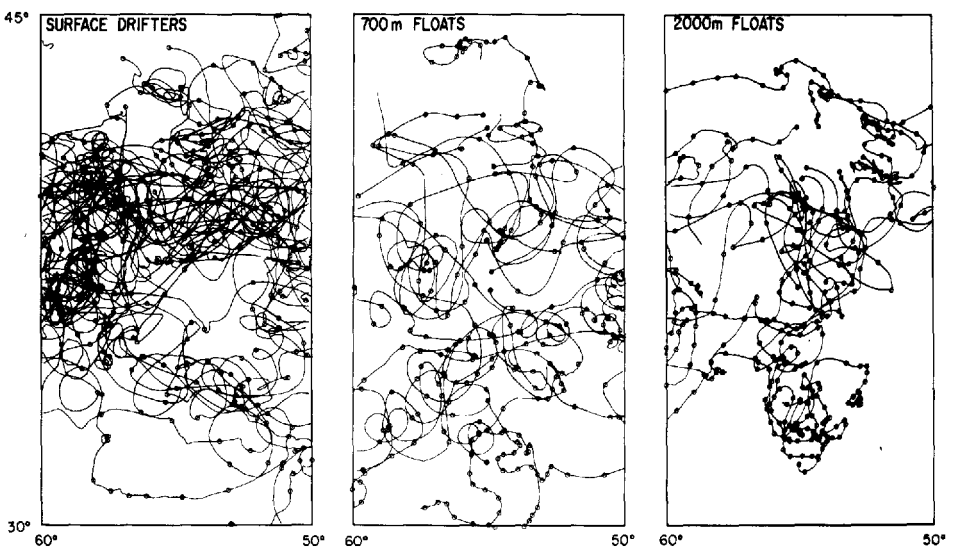

Figure 1b. Trajectories of surface drifters and SOFAR floats at 700 m and 2000 m in the study region. Drifter data are concentrated in years 1977–1980, float data are from April 1980–May 1982, and current meter data are from April 1975–July 1977.

that entered the region near 55W were also included. Floats were tracked for two years (April 1980–May 1982) by means of an array of six moored listening stations. The tracking procedure was similar to that described by Spain *et al.* (1980). The first six months of data have been discussed by Richardson *et al.* (1981), the first fifteen months of data by Owens (1984), and some of the first two years by Shaw and Rossby (1984).

Surface velocity was obtained from 49 freely drifting buoys located between 30–45N and 50–60W (Fig. 1). The buoy data are concentrated in the years 1977–1980 and are nearly evenly spaced seasonally. Satellite tracking typically obtained two fixes per buoy per day. Trajectories and velocities have been shown and discussed by Richardson (1981, 1983a, b).

Velocity of currents at 4000 m depth was obtained by moored current meters. The moorings were in place for more than two years from April 1975–July 1977. The measurement technique and results have been discussed by Schmitz (1977, 1978, 1980), Schmitz and McCartney (1982), and Schmitz and Holland (1982).

Surface buoys and subsurface floats were treated as roving current meters that gave velocity measurements along their paths. Positions and velocities were first low-pass filtered to reduce the effect of position errors and inertial and tidal fluctuations. Velocity values were then grouped into geographical boxes one degree in latitude and ten degrees in longitude, centered at 55W. The following were calculated for each box: the mean velocity $\bar{u}$, $\bar{v}$ in the x and y directions, the departures u', v' from the mean, the variance $\langle u'^2 \rangle$, $\langle v'^2 \rangle$, and the eddy kinetic energy $0.5\,[\langle u'^2 \rangle + \langle u'^2 \rangle]$. Standard error of the mean was estimated using

$$\epsilon = \left[\langle u'^2 \rangle \Big/ \left(\frac{N}{\tau} + n \right) \right]^{1/2}$$

where $\langle u'^2 \rangle$ is the variance, N is the number of daily observations, τ is the integral time scale which is assumed to be constant and equal to 8 days, and n is the number of different floats or drifters in a box. The average number of velocity observations in a 1×10 degree box in the vicinity of the Gulf Stream was approximately 500 for surface buoys, 200 for 700 m floats, and 300 for 2000 m floats.

Hydrographic sections were used to calculate an average geostrophic velocity section along 55W. Sections were selected on the following criteria: (1) they were meridional and crossed the Gulf Stream, (2) they were located within the region bounded by 51–59W, 30–45N, (3) they were high quality (salinities were reported to three decimal places), and (4) data extended from the sea surface to the sea floor (Table 1). A total of 210 stations were sorted into 1° latitude by 8° longitude boxes and values interpolated to 35 levels. The levels were spaced at 50 m from the sea surface to 400 m depth, at 100 m from 400 m to 1500 m depth, and at 250 m from 1500 m to the sea floor. Average values of temperature, salinity and oxygen were calculated for each level in each box. Individual values outside one standard deviation of the mean were

Table 1. Individual hydrographic sections used to calculate an average geostrophic velocity section along 55W.

Cruise*	Date	Longitude
1) *Crawford* 28	June 1959	57.5W
2) *Chain* 12	April 1960	52.5
3) *Chain* 12	April 1960	54.5
4) *Chain* 12	April 1960	56.5
5) *Crawford* 40	April 1960	58.5
6) *Knorr* 60	October 1976	55.0
7) *Knorr* 66	July 1977	55.0
8) *Oceanus* 133	May 1983	53.5

*Sections 2–5 are described by Fuglister (1963), sections 6 and 7 by McCartney *et al.* (1980) and Schmitz and McCartney (1982).

eliminated and averages were recalculated. Geostrophic velocity profiles were calculated between adjacent 1° latitude boxes and relative to the deepest common level.

4. Mean velocity and general configuration of currents

Figure 2 shows four profiles of mean zonal velocity at 0, 700, 2000 and 4000 m and the associated number of observations and velocity variances. Velocity values were combined and contoured on a vertical section of zonal velocity (Fig. 3a). In the following, the Gulf Stream is defined to be the eastward flow centered near 40N that is bounded by westward flow (or 44N latitude at the surface). The section shows that the average surface Gulf Stream along 55W extends from 36.0N to 44.0N, has a width of 900 km, and has a maximum surface velocity of 28 cm s^{-1} centered near 39.5N. The width of the Stream decreases with depth to about 200 km at a depth of 4000 m. The deep maximum eastward velocity at 4000 m is 6.8 cm s^{-1} centered near 37.5N, 200 km south of the maximum surface velocity. The axis of the Stream shifts southward and downward with a ratio of about 50/1.

The subsurface Gulf Stream is bounded by two westward flowing countercurrents that make it possible to clearly identify a Gulf Stream. The northern countercurrent is at least 300 km wide. It probably extends all the way to the continental shelf and slope to the north and includes the deep western boundary current, or Western Boundary Undercurrent. The northern countercurrent has peak velocities of 4–5 cm s^{-1} at 4000 m. Part of the northern countercurrent is located underneath the peak surface current of the Stream. A counterflow was not measured at the surface north of the Stream, but westward flow could exist north of 43.5N, the northernmost position at which drifter data were dense enough to resolve the mean flow.

The southern countercurrent is located between 35N and 37N and has a peak velocity of 10.9 cm s^{-1} at 4000 m. At the surface the southern countercurrent is seen only as a minimum (at 35.5N) in the predominantly eastward flow there. The southern countercurrent is bounded on its south by a generally eastward flow between 33 and

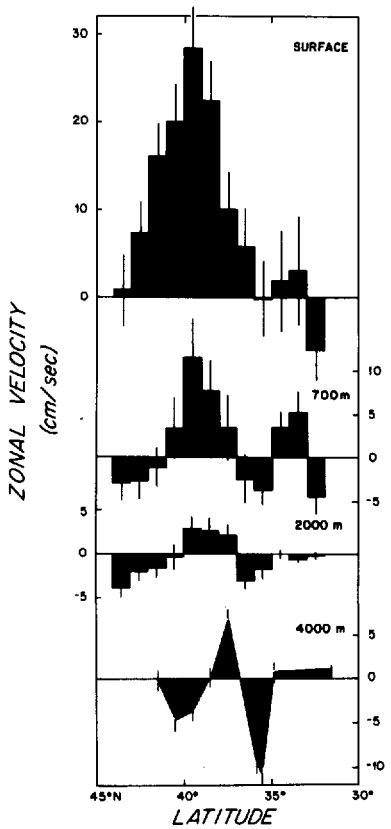

Figure 2a. Mean zonal velocity across 55W from surface drifters, SOFAR floats at 700 m and 2000 m, and current meters at 4000 m. Mean velocity was calculated from drifter and float data by grouping individual measurements into boxes one degree in latitude by ten degrees in longitude. Error bars represent estimates of the standard error of the mean.

35N, although the velocity at 2000 m is weak and westward there. South of this, at 32.5N, westward flow is observed at the surface, 700 m, and 2000 m.

A section of eddy kinetic energy (Fig. 3b) shows that the Gulf Stream and its bounding countercurrents coincide with a region of high eddy energy and its gradient. The general patterns of zonal currents and eddy energy seen here are strikingly similar to the results of some recent eddy-resolving general circulation models (Holland, personal communication); the patterns are kinematically and dynamically linked.

Several current meter moorings are as shallow as 600 m in the southern edge of the Gulf Stream and in the southern countercurrent (Schmitz, 1980). The mean velocities from these agree with the float velocities in showing narrow, vertically coherent zonal currents (see Owens, 1984). The remarkable agreement between the two data sets made during different periods of time indicates that we are observing real features of the long-term mean velocity field. The weak depth-dependence of currents (below

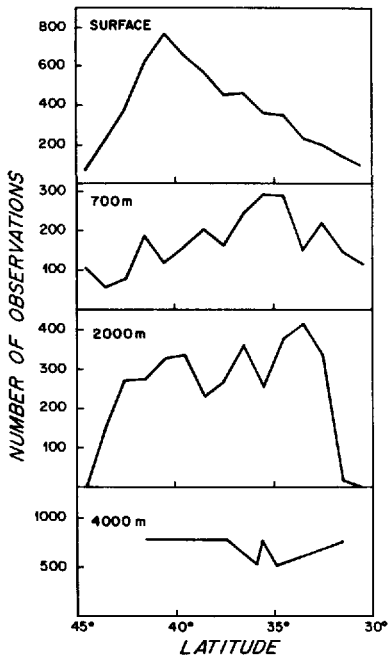

Figure 2b. Number of daily observations (semi-daily for drifters) in each box.

700 m) and their strong vertical coherence suggest that the Gulf Stream and countercurrents extend coherently downward to the sea floor. Hydrographic data support this conclusion, since little mean vertical shear is observed in geostrophic profiles in deep water.

Confirming evidence of the three deep currents (the Gulf Stream and two countercurrents) is provided by three 9-month (nominal) mean velocity profiles from the current meter moorings (Fig. 4). Although there were variations in the magnitude and location of the three deep currents (and their vertical shear), all three could be clearly identified on each 9-month record. The dominant variation was a large scale, ~200 km, southward shift in the position of the deep Gulf Stream over 18 months.

Mean velocity was greater at 4000 m than at 2000 m. This difference is probably a result of the different kinds of averages used. The space-time averages of float data tend to smooth over what could be higher time-average currents with short space scales. The mean velocities along 55W have been interpreted here as large-scale zonal currents. Supporting evidence is the agreement of current meter and float measurements made at different times. However, a topographic bump 400 m high near 36N, 55W biased the current meter velocities. Using the current meter records from the third setting, Owens and Hogg (1980) found evidence that a significant portion of the deep flow near 36N was going around the bump in an anticyclonic direction. The anticyclonic eddy is trapped in the deep layer, but it coincides with the upper layer

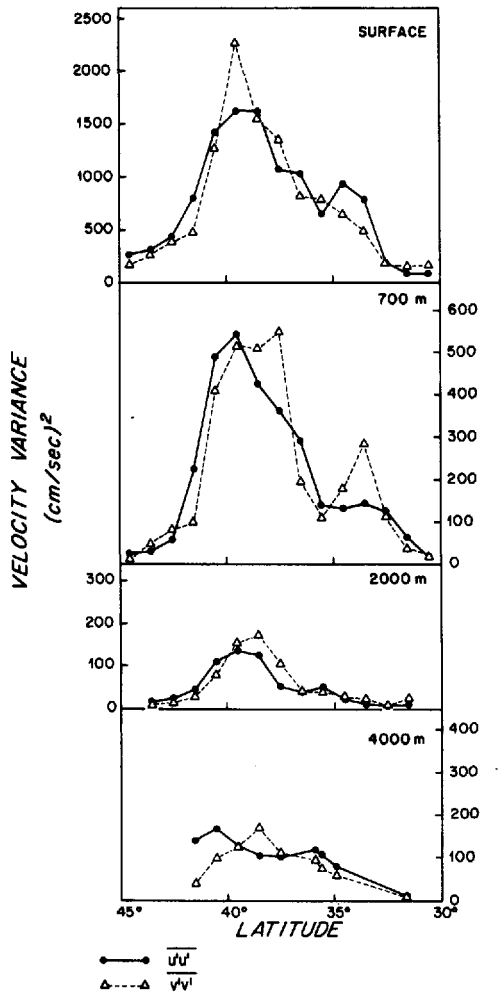

Figure 2c. Velocity variance about the mean velocity in each box.

crossover between eastward Gulf Stream and westward countercurrent flow near 36N. This explains the large amplitude of mean velocity in the southern countercurrent and the large amplitude of eastward flow at 36.5N on the third setting. The size of the bump and the inferred eddy suggest that the velocity in the deep Gulf Stream near 37.5N was probably not significantly biased by flow around the bump.

Grouping velocities from floats and buoys and calculating space-time averages circumvents the topographic problem by averaging over small-scale features. However, space-time averaging has the potential disadvantage that narrow features, such as the deep Gulf Stream and countercurrents, could become overly smoothed or blurred—especially if there are significant geographical variations within a box. Near 55W, the

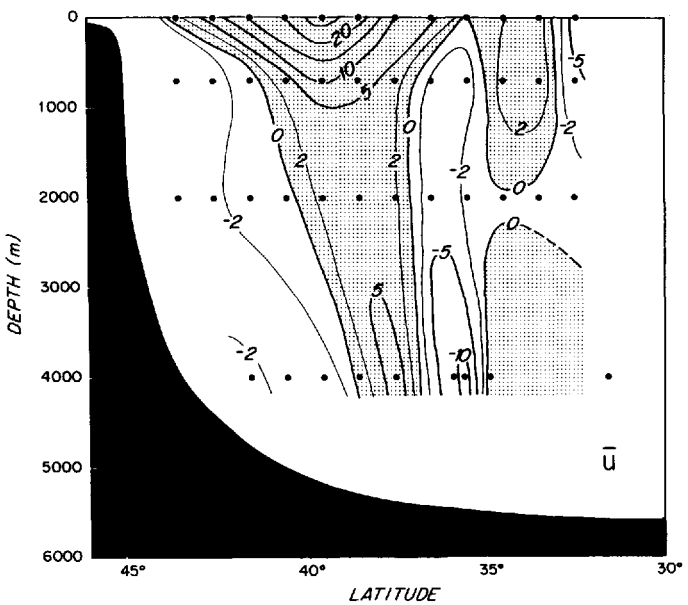

Figure 3a. Contoured zonal velocity section (cm s^{-1}) along 55W and through the Gulf Stream from drifters, floats, and current meters. Eastward velocity is shaded. Dots indicate centers of boxes used in calculating velocity except at 4000 m, where they show current meter locations. The bottom profile is from 55W; the average bottom profile between 50–60W is shifted southward from this by about one degree in latitude (see Fig. 1a).

average near-surface Gulf Stream appears to run almost exactly eastward (Wyrtki *et al.*, 1976; Emery, 1983; Robinson *et al.*, 1979); the mean direction of the surface jet from drifters is 93° (see Fig. 1a). The mean Gulf Stream is also nearly eastward—92° at 700 m, 86° at 2000 m, and 92° at 4000 m. Therefore, this problem is probably not important here. Larger boxes, two degrees in latitude, resulted in more observations per box and a higher statistical accuracy, but the increased size tended to blur the deep Gulf Stream and countercurrents. Calculations were repeated in one-degree boxes that had been shifted northward half a degree. Although the velocity profiles varied somewhat from the first set of calculations, there was good agreement in the main features and in estimates of transport.

5. Geostrophic velocity

Figure 5 shows a section of average zonal velocity across 55W calculated from historical hydrographic data with the geostrophic relation and by assuming zero velocity at the sea floor. Because this figure only shows velocity relative to the bottom and not absolute velocity, the deep Gulf Stream and countercurrents which are nearly barotropic (Fig. 3a) do not appear. Despite this problem, there are some similarities

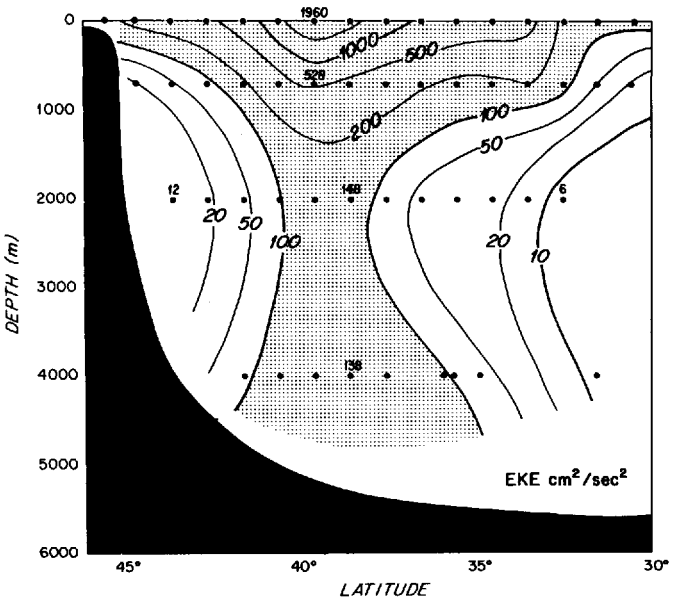

Figure 3b. Contoured section along 55W of eddy kinetic energy (per unit mass). Units are $cm^2\ s^{-2}$. High eddy kinetic energy and its gradient coincide with the mean Gulf Stream and bounding countercurrents.

between the geostrophic velocity (Fig. 5) and directly measured velocity (Fig. 3a). The upper level Gulf Stream is similar; it is centered near 39N and has the same approximate width. The largest deep shear under the surface Stream is also located near 39N. The Stream is bounded on the south by a countercurrent centered near 35N.

A slight minimum in eastward geostrophic velocity is located at 41N. The northern band of current centered near 42N is called the Slope Water Current by Fuglister (1963) who thought it was a separate current. Since it is connected to the Stream in Figure 5 and merges completely with the Stream in the direct velocity section (Fig. 3a) the current will be considered part of the Gulf Stream here. Because one half of the eight hydrographic sections used to obtain the geostrophic section (Table 1) are from Fuglister's (1963) experiment, the geostrophic section is strongly based on his data.

The southern limit of many of the hydrographic sections including Fuglister's (1963) was 33N, and the number of stations south of this latitude was greatly reduced. Thus the "eddy" or crossover from east velocity to west velocity at 32.5N could be due to this discontinuity in synoptic data. The shear in the southern countercurrent has different signs in Figures 5b and 3a. Part of this difference can be explained by (1) an inflated current meter velocity at 4000 m due to the topographic bump as described above and (2) a reduced drifter velocity at the surface due to local surface wind-driven velocity and which will be discussed below.

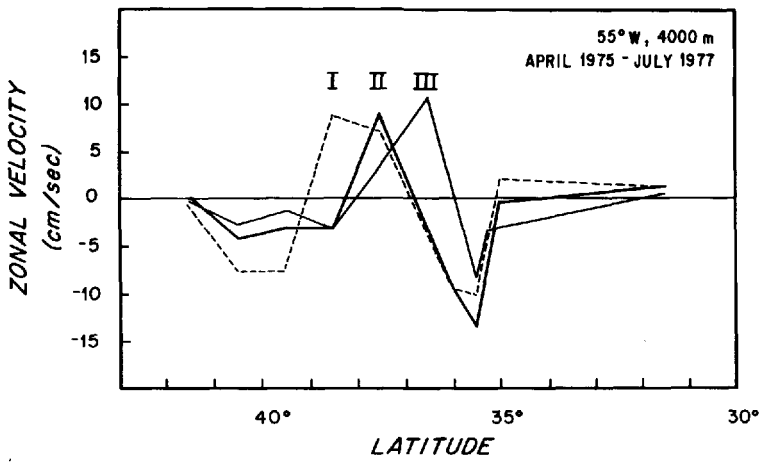

Figure 4. Velocity profiles along 55W at a depth of 4000 m based on the three nine-month deployments of Polymode Array II (May 75–December 75, December 75–October 76, and October 76–July 77) as given by Schmitz and McCartney (1982). The deep eastward flow in the Stream shifted approximately 200 km southward over an 18 month period. Note that all three profiles show a deep Gulf Stream bounded by two countercurrents. Only on the third deployment was a current meter placed at 36.5N.

6. Surface velocity

Three meridional profiles of average eastward surface velocity across 55W are shown in Figure 6a. One profile is from surface drifters, a second is from average ship drift velocities (data were obtained from the U.S. Naval Oceanographic Office), and the third is from geostrophic calculations. The three agree astonishingly well in showing the size, shape and velocity of the Gulf Stream. The implication is that the surface drifters have resolved the long-term mean velocity. One significant difference in profiles is the swift southern countercurrent near 35N in geostrophic velocity. The drifter and ship drift profiles only indicate a minimum near 35.5N in predominantly eastward velocity. (South of 33N the number of observations is low and profiles are noisy.) The explanation of this discrepancy concerns the average wind velocity near the Gulf Stream at 55W which is eastward with a magnitude of about 3 m s^{-1} (Bunker and Goldsmith, 1979). The wind drives a surface velocity called wind drift velocity here with an eastward component of about 3–4 cm s^{-1} (Fig. 6a).

A profile of eastward wind drift velocity across 55W was estimated using the empirical relationship reported by McNally (1981). His drifting buoys in the eastern North Pacific moved systematically 35° to the right of the near-surface wind at a speed of 1.45% of the wind speed. These values were coupled with the mean wind velocity along 55W given by Bunker and Goldsmith (1979) to produce the profile of zonal wind drift velocity shown on Figure 6a. The real response of the ocean to wind forcing is complicated and depends on many factors. The estimates above are thus only a crude

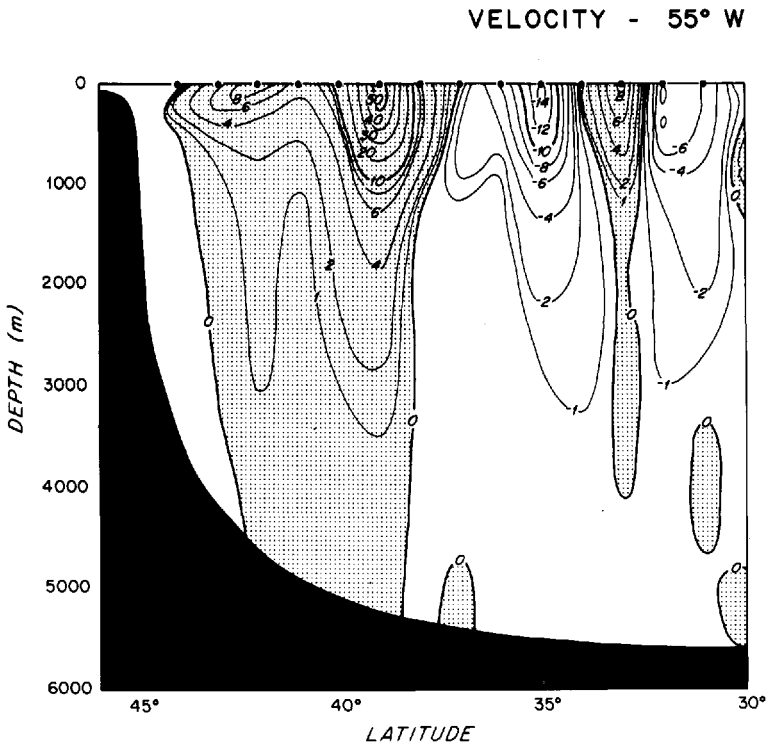

Figure 5. Geostrophic velocity across 55W based on the average hydrographic section and by assuming zero velocity at the sea floor. Dots indicate locations of velocity profiles.

approximation of the real time-mean wind-driven surface current. In these estimates the slippage of the buoys through the water is considered small compared to the wind-driven current and has been neglected (see McNally, 1981; and Richardson, 1983b).

This wind drift velocity augments the geostrophic velocity in the Gulf Stream and diminishes the geostrophic velocity in the countercurrents. When the eastward wind drift velocity is subtracted from the surface velocity calculated from either buoys or ship drifts, the southern countercurrent (and northern one too) is apparent (Fig. 6b). Ship drifts show the northern countercurrent north of 44N with a westward velocity of 6 cm s^{-1} at 44.5N. Ship drifts and buoys show the southern countercurrent centered near 36N with a westward velocity of 4 cm s^{-1}.

A second possible explanation of the broad surface Gulf Stream concerns the space-time averaging procedure. On a synoptic time scale, the peak surface Gulf Stream velocity is much swifter than that of the countercurrents. The combination of such a swift current and its broad meander pattern (Fig. 1a) would tend to overwhelm the countercurrents in space-time averaging.

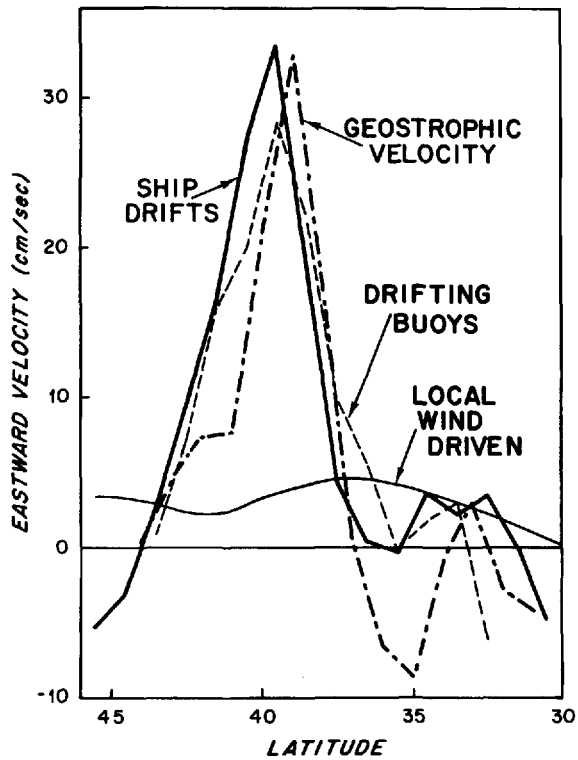

Figure 6a. Surface zonal velocity across 55W from drifting buoys, historical ship drifts, geostrophic calculations using historical hydrographic data, and local winds. The geostrophic velocity profile was smoothed spatially with a filter whose weights are ¼, ½, ¼ in order to reduce some small scale, 1 degree, latitude variations. The wind drift velocity was estimated by using a factor of 1.45 percent of the magnitude of the mean wind vector (Bunker and Goldsmith, 1979), and was rotated to 35° to the right of the direction of the mean wind vector (see McNally, 1981). The effect of the local wind drift current is to augment velocity in the Gulf Stream and to diminish the eastward velocity in the countercurrents bounding the Stream.

7. Mean transport

a. Gulf Stream. Estimates of the volume transport of the Gulf Stream were made by (1) integrating latitudinally the velocity data at the four depths—0, 700, 2000, and 4000 m, (2) assuming different relationships of transport per unit depth, and (3) integrating vertically (Fig. 7, Table 2). The total transport of the champagne glass shaped Stream from linear interpolation is 99×10^6 m^3 s^{-1}. This consists of all the eastward transport between 36–44N at the surface and between the two countercurrents below the surface. A second estimate, 88×10^6 m^3 s^{-1}, was made by passing straight lines through the upper two values and lower two values. A third and better estimate was made by passing a smooth curve through the four values and extrapolat-

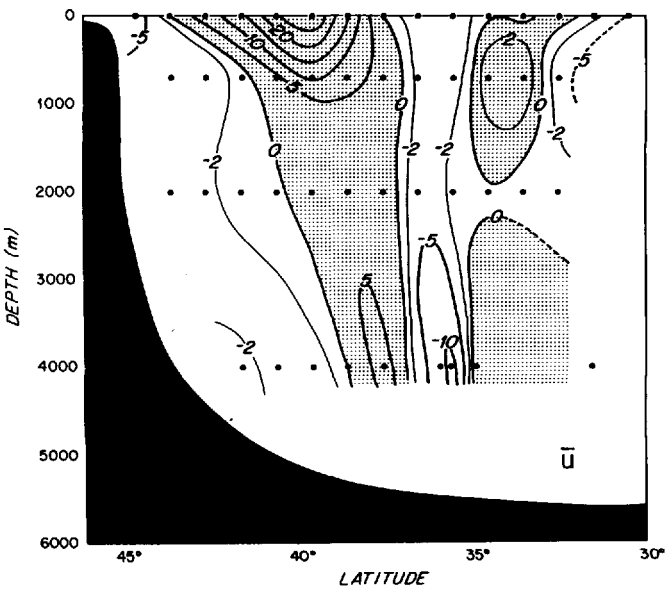

Figure 6b. Contoured zonal velocity section (cm s^{-1}) along 55W with the wind drift velocity removed. Surface velocity was obtained by subtracting the local wind drift component from the mean velocity calculated from shift drifts. Below the surface values are the same as shown in Figure 3a.

ing it to the sea floor. This gives a transport of 93 × 10^6 m^3 s^{-1}. The standard error of transport was estimated to be 11 × 10^6 m^3 s^{-1} by combining the standard errors of the values from the boxes and current meters.

The value thus obtained (93 × 10^6 m^3 s^{-1}) is noteworthy in that it is the first long-term, direct measurement of mean transport from surface to bottom in deep water. Approximately 34 × 10^6 m^3 s^{-1}, or 37 percent of the total transport, is independent of depth—a barotropic transport. It is this barotropic component that has been impossible to measure with hydrographic data alone. The total transport is close to the value of average geostrophic transport calculated relative to zero velocity at the sea floor along 55W which is 88 × 10^6 m^3 s^{-1}. However, the structure of the average transport across 55W is considerably different from the geostrophic transport due to the presence in the mean of significant barotropic transport.

The measured surface transport value (per unit depth) includes the local wind drift velocity. Since the surface mixed layer is about 50 m thick, we need to use the real shape of the transport—depth relationship to estimate the correction (or error) to the previous integrated transport value. The correction is about −8 × 10^6 m^3 s^{-1} and was estimated as follows: (1) the estimated wind drift velocity was obtained by combining the mean wind vectors from Bunker and Goldsmith (1979) and transfer coefficients given by McNally (1981) as already described. (2) This zonal velocity was subtracted

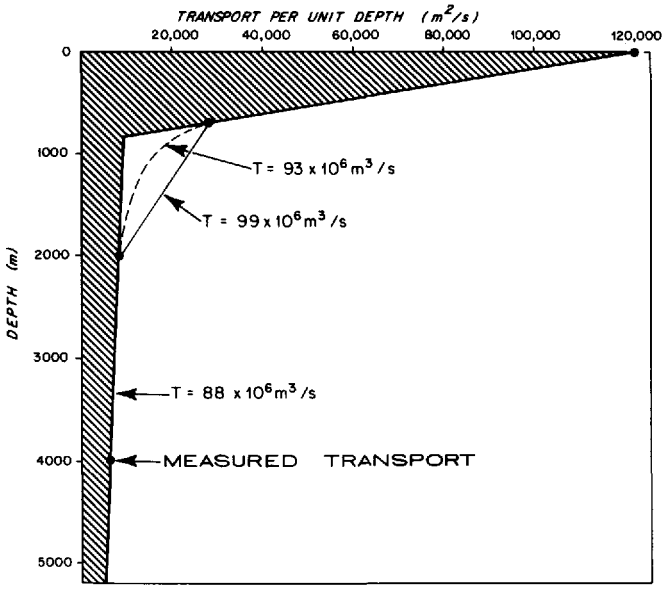

Figure 7a. Mean zonal transport profile of the Gulf Stream along 55W. Values were obtained by integrating the eastward velocity bounded by countercurrents at each of the four levels (Fig. 2a). The total surface-to-bottom transport, estimated by using linear interpolation between the four levels and extrapolating a constant value below 4000 m, is 99 × 10^6 m^3 s^{-1}. Using two straight lines fitted to the two upper and two lower values gives a transport of 88 × 10^6 m^3 s^{-1}. Using a smooth curve gives 93 × 10^6 m^3 s^{-1}.

from the velocity calculated from the drifters (see Fig. 6a). (3) The result was integrated horizontally and combined with the transport profile as before to obtain a new total integrated transport. (4) Finally, the estimated zonal wind drift velocity was multiplied by a depth of 50 m and added back to give a total transport, of 85 × 10^6 m^3 s^{-1}. The 50 m mixed layer was assumed to move as a slab as described by McNally (1981). Because of the many assumptions used, the correction of 8 × 10^6 m^3 s^{-1} is only a crude estimate of how much the Gulf Stream transport should be reduced.

The estimate of total mean transport of the Gulf Stream depends strongly on the value of 4000 m, since this value represents the lower 2 km or 40% of the water column. Two problems encountered when estimating transport from the deep current meter velocities were: (1) only one meter was located in the deep mean Stream, making it difficult to estimate the real across stream velocity profile, (2) the deep Stream made a large-scale long-period north-south shift during the two-year deployment which raises questions about the representativeness of the two-year mean velocity.

Having only one meter in the deep Gulf Stream tends to underestimate mean transport there. To evaluate the size of this error, an estimate was made of the effect of having another current meter in the deep Stream near 36.5N. Only during the third

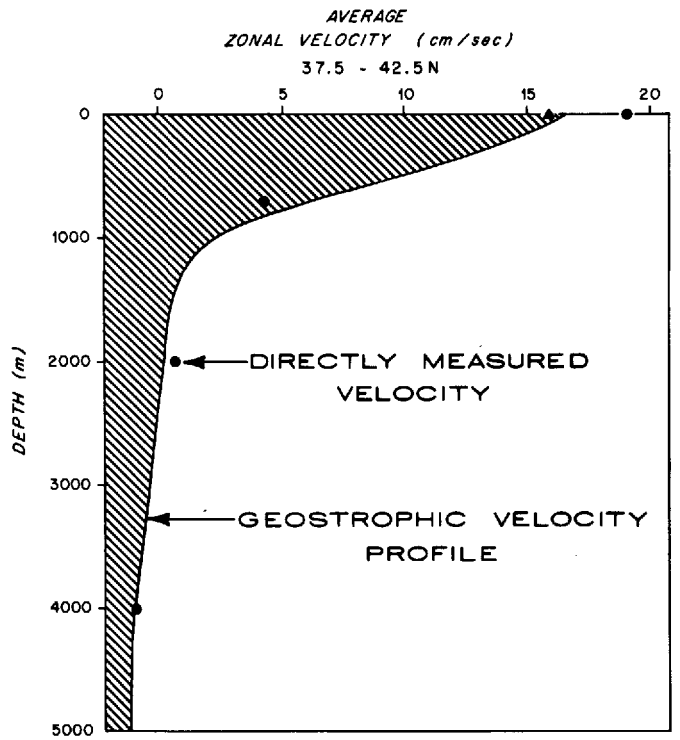

Figure 7b. Geostrophic velocity profile and measured velocity values averaged over the latitude band 37.5–42.5N. The profile was adjusted to pass through the directly measured value at 4000 m. The triangle indicates the surface value corrected for wind drift velocity.

Table 2. Summary of measured transport in the Gulf Stream, Northern Countercurrent and Southern Countercurrent across 55W.

	Transport per unit depth (10^3 m^2 s^{-1})		
Depth	Northern Countercurrent	Gulf Stream	Southern Countercurrent
Surface (buoys)	0 ± 4	122 ± 13	0 ± 5
700 m (floats)	7 ± 4	28 ± 8	7 ± 4
2000 m (floats)	9 ± 2	8 ± 3	5 ± 2
4000 m (current meters)	9 ± 2	7 ± 1	12 ± 1
	Total Transport (10^6 m^3 sec^{-1})		
Surface-bottom	41 ± 8	93 ± 11	42 ± 6

The total Gulf Stream transport, 93 × 10^6 m^3 s^{-1}, was obtained by passing a smooth curve through the four measured values, and vertically integrating the results. Values at 4000 m were determined from current velocities given by Schmitz (1980).

The total transport of the countercurrents was estimated using linear interpolation between the four measured values and a constant transport between 4000 m and the sea floor.

The uncertainty in transport was calculated by combining the standard errors from the boxes and current meters. It was assumed that the mean velocity in each box or at each current meter has a standard error that is uncorrelated with the standard error of adjacent boxes or current meters.

Table 3. Transport at 4000 m based on three current meter deployments.

	Transport per unit depth (10^3 m^2 s^{-1})		
Deployment	Northern Countercurrent	Gulf Stream	Southern Countercurrent
First (May 75–Dec 75)	15	14	12
Second (Dec 75–Oct 76)	10	8	14
Third (Oct 76–Jul 77)	7	13	10
Total (May 75–Jul 77)	9	7	12

Transport values were estimated using the three sets of zonal velocities from current meters at 4000 m as given by Schmitz and McCartney (1982) and shown in Figure 4. On the third deployment only a current meter was moored at 36.5N in the deep Gulf Stream.

deployment was a meter actually there—one that recorded a strong mean eastward velocity of 10.7 cm s^{-1}. This value is probably an overestimate due to the topographic bump discussed previously. If we use this velocity plus values linearly interpolated to this latitude from velocity profiles on the first two deployments, we obtain a 27-month estimated mean eastward velocity at 36.5N of about 2 cm s^{-1}. A recalculation of the 27-month mean transport at 4000 m including this value gives a transport of about 9×10^3 m^2 s^{-1}, an increase of about 2×10^3 m^2 s^{-1} over the earlier 27-month value. (This new value is in accord with the transport at 2000 m calculated from float data.) The 9×10^3 m^2 s^{-1} is thus an estimate of transport that might have been calculated if two current meters rather than one had been located in the mean deep Gulf Stream. If we use the additional transport as an estimate of the characteristic uncertainty in transport per unit depth, and multiply it by the total water depth, we obtain a value of about 10×10^6 m^3 s^{-1} as the uncertainty of total volume transport of the Gulf Stream (or 4×10^6 m^3 s^{-1} over the lower 2 km).

The time variability of transport at 4000 m can be estimated from each of the 9-month current meter deployments. The three values are 14, 8, and 13×10^3 m^2 s^{-1} (Table 3). Note again that the third value is partly based on an additional meter at 36.5N that was probably influenced by local topography. Although there are variations of about a factor of two between these three estimates, they agree in general. At no time does the deep Gulf Stream (or either countercurrent) disappear. To estimate the long-term average transport, we used the 27-month average, 7×10^3 m^2 s^{-1}. One reason this value is smaller than the average of the three separate estimates concerns the countercurrents bounding the deep Stream. When these currents shift north or south, a long-term mean velocity near the edge of the Stream includes a combination of eastward and westward flow. Presumably, as even longer time averages of deep currents are obtained, the apparent mean transport of the Stream (and countercurrents) will decrease further. Conversely, shorter time averages would increase the apparent transport, at least down to mesoscale periods.

b. Countercurrents. The total transport of the northern countercurrent, estimated by linear interpolation of the four measured values, is 41×10^6 m^3 s^{-1}. This consists of all the westward flow north of the Gulf Stream. At 700 m, the velocity values of 2.7 and 2.8 cm s^{-1} at 42.5 and 43.5N were used despite a relative scarcity of observations at these locations. These values agree with values at 2000 m and 4000 m. Excluding them would decrease the estimated transport by about 5×10^6 m^3 s^{-1}. North of about 42N and near 50W, the boxes used to calculate the velocities intersect the continental shelf and slope, making the meaning of average zonal velocity problematic. If we arbitrarily exclude the northernmost velocity values (centered at 43.5N, 700 m and 2000 m) the transport of the countercurrent decreases by about 10×10^6 m^3 s^{-1}. The estimated correction to the total transport related to wind drift velocity, as discussed earlier, is about $+2 \times 10^6$ m^3 s^{-1} for the northern countercurrent.

The transport of the southern countercurrent, the westward transport between 35N and 37N, is 42×10^6 m^3 s^{-1} based on linear interpolation. However, the estimated transport per unit depth at 4000 m is about twice as large as values at 700 m and 2000 m (Table 2). This is due to excessively large westward velocity at 35.5N, associated partly with the anticyclonic circulation around the bump described earlier. If the 4000 m transport is halved to bring it in line with transport values at lesser depths, then the total volume transport of the southern countercurrent is reduced by about 13×10^6 m^3 s^{-1}. This value is about the same as the estimated anticyclonic transport around the bump in the lower 2 km, as inferred by Owens and Hogg (1980). Thus the best estimate of total zonal transport of the southern countercurrent is $42 - 13 = 29$ (all $\times 10^6$ m^3 s^{-1}). The estimated correction associated with the wind drift velocity is again about $+2 \times 10^6$ m^3 s^{-1}. The geostrophic transport of the southern countercurrent between latitudes 33.5N and 37.5N is 34×10^6 m^3 s^{-1}.

Schmitz (1980) has estimated the transport of the southern countercurrent to be 70×10^6 m^3 s^{-1}. He used current meter data at 600, 1500, 2000, and 4000 m and extrapolated values to the surface and bottom. The transport estimated in this paper is smaller because (1) the mean velocity and transport at 700 m and 2000 m measured by floats are smaller than those measured by current meters and (2) the measured surface value is much smaller than Schmitz's extrapolated value, 22 cm s^{-1}.

8. Discussion

Our estimate of the volume of water transported by the Gulf Stream, 93×10^6 m^3 s^{-1}, is considerably smaller than values given by several others for this same general region (Fuglister, 1963; Barrett and Schmitz, 1971; Clarke and Reiniger, 1973; Robinson *et al.*, 1974; Worthington, 1976). These earlier estimates are measurements of the instantaneous or synoptic transport of the Stream, values that depend critically on the meander pattern and distribution of eddies and countercurrents at the time measurements are made and on the method of combining direct velocity and

Table 4. Volume transport of the Gulf Stream.

	Reported by	Method	Date	Location (km from Miami)	Longitude	Transport (10^6 m^3 s^{-1})
1	Niiler and Richardson (1973)	T	1964–1970	0		30
2	Richardson *et al.* (1969)	T	June, Aug 1966 May, June 1967	210		33
3	Richardson *et al.* (1969)	T	May, June 1967	300		35
4	Richardson *et al.* (1969)	T	May, June 1967	530		37
5	Knauss (1969)	T	Sept 1966	725		52
6	Richardson *et al.* (1969)	T	June, July 1968	910		55
7	Swallow and Worthington (1961)	G	March 1957	980		64
8	Knauss (1969)	T	July, Aug 1965	1050		57
9	Richardson and Knauss (1971)	T	July 1967	1215		63
10	Barrett (1965)	G	Oct 1962	1225		60
11	Worthington and Wright (Knauss, 1969)	G	Nov 1966	1315		74
12	Knauss (1969)	T	July, Aug 1965	1400		76
13	Robinson *et al.* (1974)	G	July 1969	1760	70.0	227
14	Warren and Volkmann (1968)	G	June 1966	1840	69.3	101
15	Barrett and Schmitz (1971)	T	June, July 1968	2020	67.3	166
16	Fuglister (1963)	G	May, June 1960	2270	64.5	147
17	Richardson (present work)	BFCM	1975–1982	3110	55.0	93
18	Clarke *et al.* (1980)	G	May 1972	3530	49.8	79
19	Clarke and Reiniger (1973)	G	June 1970	3550	49.5	130

T designates estimates based on transport floats that measure the vertically integrated horizontal velocity. G designates estimates based on geostrophic velocity from hydrographic sections, and neutrally buoyant floats (except for number 18 which used zero velocity at the sea floor and 13 and 19 which used current meters). BFCM designates an estimate of average transport using buoys, floats, and current meters.

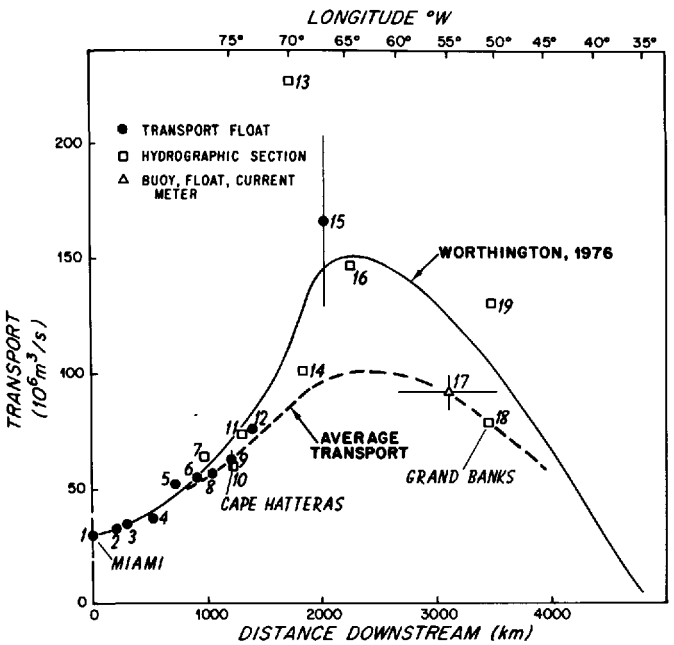

Figure 8. Variation of transport of the Gulf Stream as a function of distance downstream from Miami. Values are listed in Table 4. The vertical lines near 0, 1200, and 2000 km show the range of transport values at these locations. The solid curve represents the variation of synoptic transport as given by Worthington (1976). The dashed curve shows the variation of time-average transport; this curve passes through a directly measured value near Cape Hatteras and the time-average value at 55W and follows the approximate shape of the synoptic transport curve.

geostrophic velocity. The transport estimate given here is more representative of the long-term mean, because it is based on space-time averages of velocity (time averages for current meters). These provide an average of the time-dependent current fluctuations. The mean transport is a quantity that should be used when comparing the real Gulf Stream to time averaged model Gulf Streams.

The only other similar average transport values are from the Straits of Florida and along the coastal margin south of Cape Hatteras (Table 4, Fig. 8). Compared with 30×10^6 m^3 s^{-1} transport at the Straits of Florida the mean transport of the Stream doubles by the time it has reached Cape Hatteras and may treble farther downstream. The mean transport of the Gulf Stream along 55W is nearly equivalent to the baroclinic transport, although the vertical distributions are different due to a mean barotropic component.

The sum of westward transport in the countercurrents north of 35N is 70×10^6 m^3 s^{-1} (Table 5), more than enough to recirculate locally the northward increase in

Table 5. Transport budget across 55W north of 35N (10^6 m^3 s^{-1})

	Northern Countercurrent	Gulf Stream	Southern Countercurrent 35–37N	Net (Eastward)
Total surface to bottom transport	−41 (−2)	93 (88)	−29 (−36)	23 (51)
Total corrected for wind drift velocity	−42	85	−31	11
Upper layer transport (0–700 m)	−3 (−1)	54 (55)	−3 (−15)	48 (39)
Upper layer corrected for wind drift velocity	−4	45	−5	36
Lower layer transport (700–bottom)	−38 (−1)	40 (33)	−27 (−21)	−25 (11)

Transport values (rounded to nearest 10^6 m^3 s^{-1}) were calculated using linear interpolation between the four measured values, except for the Gulf Stream, where the value is based on the smooth curve fitted to observed values. The southern countercurrent is reduced by 13 × 10^6 m^3 s^{-1} from its value in Table 2 to correct for transport circulating around a topographic bump near 35N, 55W. Values in parenthesis are transport estimates from average geostrophic velocity profiles relative to zero velocity at the sea floor. The southern limit of the southern countercurrent in the geostrophic transport estimate is 33.5N. The net geostrophic transport across the whole section from 29.5 to 44.5N is 36 × 10^6 m^3 s^{-1} (eastward).

Gulf Stream transport. To examine the balance of transport, values were subdivided into upper and lower layers (Table 5), using as a dividing line 700 m, the maximum depth of the Florida Straits and the depth above which the transport per unit depth increases rapidly along 55W (Fig. 7). Below 700 m, transport values in each current are nearly constant with depth.

A crude transport budget for the region north of 35N along 55W is as follows, in units of 10^6 m^3 s^{-1}:

(1) In the upper layer, the Gulf Stream transport is 45–54 (depending on whether or not the correction for wind drift velocity is included). Of this, 6–9 is recirculated locally in the countercurrents, 30 is returned over the subtropical gyre, and some 6–18 continues northeastward in the North Atlantic current.

(2) In the lower layer, the Gulf Stream transports 40 eastward. The northern countercurrent transports 38 westward, but 10–15 of this is the Western Boundary Undercurrent, a net westward flow through the region (see Richardson, 1977; Hogg, 1983). The southern countercurrent transports 27, but part of this could be recirculated eastward south of 35N. Thus 23–28 of the deep Gulf Stream transport is recirculated in the northern countercurrent and 12–17 in the southern countercurrent. If we lower the transport of the northern

countercurrent by 5 to correct for a possible overestimate of transport as discussed earlier, then the recirculation carried by each countercurrent equals approximately 20. The actual deep Gulf Stream transport is possibly larger than 40 (the underestimate is due to having only one current meter). Larger transport would help bring the deep values into closer balance.

This transport budget is, of course, very tentative because of the large uncertainties in transport estimates and other problems noted above.

The picture of general circulation from these data is a Gulf Stream flanked by countercurrents that recirculate all of the Stream's deep transport and 10–20% of the upper layer. The budget suggested here differs from Worthington's (1976) values along 55W in that

(1) he has a larger total Gulf Stream transport (125) all of which is recirculated in the subtropical gyre,

(2) none of his Gulf Stream recirculation occurs north of the Stream, although he shows an anticyclonic circulation of 15 there between the Western Boundary Undercurrent and Stream, and

(3) his transport estimate of the Western Boundary Undercurrent is 8, smaller than that used here.

The inferred deep circulation consisting of the Western Boundary Undercurrent and the counter-rotating gyres agrees with a map of deep currents given by Hogg (1983). This map was based on a larger set of deep current meter measurements. Hogg adds the zonal dimension and concludes that the zonal scale of the Gulf Stream-countercurrent system is 15–20 degrees in longitude, much larger than the meridional scale.

Final balancing of eastward and westward transport through sections like 55W, and the drawing of the three-dimensional circulation patterns, must await more data. Needed are both more geographical coverage to complete the velocity section, and more quantity and quality of measurements to increase the accuracy of velocity and transport determinations.

Acknowledgments. This is contribution 5623 from the Woods Hole Oceanographic Institution. Funding was provided by the National Science Foundation Grant OCE81-09145. W. J. Schmitz, Jr. initiated the SOFAR float work in the Gulf Stream along 55W and provided the deep current meters data. J. R. Valdes supervised the construction and launching of SOFAR floats and listening stations; H. T. Rossby tracked the floats at the University of Rhode Island; T. K. McKee processed and plotted the data; D. Carson drafted the figures; and M. A. Lucas typed the manuscript. M. McCartney and M. Raymer kindly provided the hydrographic data along 55W and C. Wooding generated the sections. An earlier version of this manuscript was written while the author was a visiting scientist at the Centre Oceanologique de Bretagne in Brest. Arrangements for this visit were made by Alain Colin de Verdiere, and support was provided by the Centre National pour l'Exploitation des Oceans.

APPENDIX

Biproducts of calculating an average geostrophic velocity section are sections of average hydrographic properties. Since these give information about the location and origin of specific water masses along 55W they are included here with a brief description. More complete descriptions of the water properties in the western North Atlantic are given by Fuglister (1963), Barrett (1965), Worthington and Wright (1970), Wright and Worthington (1970), Worthington (1976), Clarke *et al.* (1980), and McCartney *et al.* (1980).

Potential temperature

The main thermocline as denoted by the 10C isotherm is nearly level except for two locations where it (1) rises abruptly toward the north near 39N and (2) surfaces near 42.5N (Fig. 9a). These two latitudes correspond to the two maxima in eastward geostrophic velocity (Fig. 5). In the deeper water, >2000 m, the isotherms are bowl-shaped and slope up toward the north and south from a maximum depth near 38N at the southern flank of the Stream. Major exceptions are the 3.4 and 3.6C isotherms which dip down toward continental slope near a depth of 1800 m. The northward spreading of the 3.6 and 3.8C isotherms centered near 1500 m indicates a region of nearly isothermal water which has anomalously low salinity.

Salinity

The near-surface salinity ranges from a maximum of 36.7‰ near 30N to a minimum of 32.1‰ near 45N (Fig. 9b). The isohalines in the main thermocline and also those below 3000 m closely follow the isotherms. Southward spreading of 35.0‰ and 35.2‰ isohalines near 1200 m and south of 37N indicates the salty Mediterranean water influence. The northward spreading of 34.94 and 34.96 isohalines near and above 2000 m adjacent to the Slope indicates low salinity water.

Salinity anomaly

The salinity anomaly is the difference in salinity at a given potential temperature between the average observed salinity and the standard potential temperature salinity relation for the western North Atlantic given by Worthington and Metcalf (1961) for temperatures less than 4C, by Iselin (1936) for temperatures 4–18C, and by Fuglister (personal communication) for temperatures warmer than 18C.

The dominant positive anomaly is the Mediterranean Water centered at 1200 m near 30N (Fig. 9c). This maximum which lies near 6C extends northward to the central Gulf Stream near 40N. Between 35N and 40N which includes the Stream and southern countercurrent, the distribution is quite patchy. This could be due to entrainment into the Stream farther west of Mediterranean Water and its subsequent advection eastward. It could also be due to lateral shifts of the Stream coupled with the inherent patchiness of the Mediterranean Water in this region.

North of 40N and shallower than 2700 m is a broad region of anomalously fresh water (with a near surface southward extension at temperatures warmer than 15C).

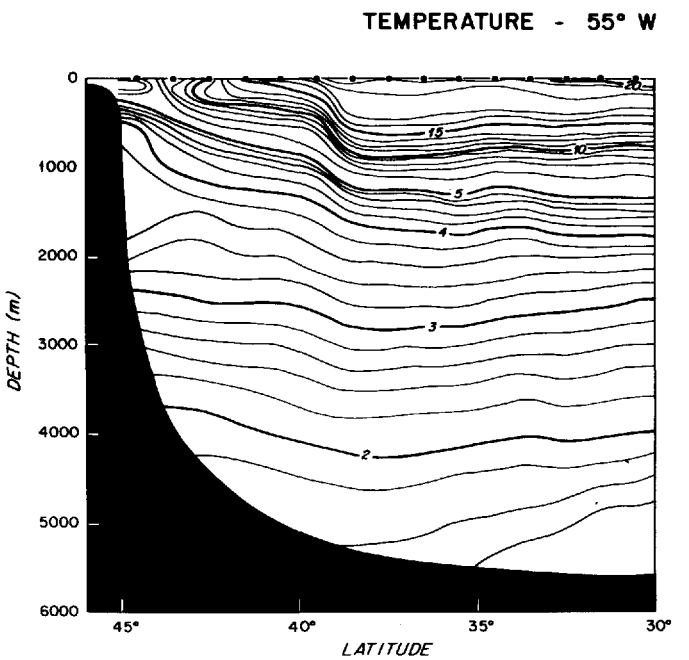

Figure 9a. Section of average potential temperature (°C) along 55W.

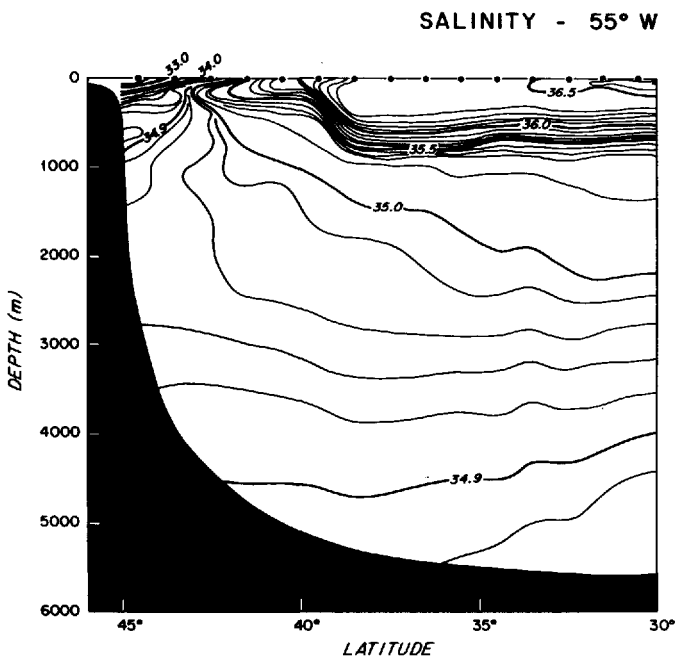

Figure 9b. Section of average salinity (‰) along 55W.

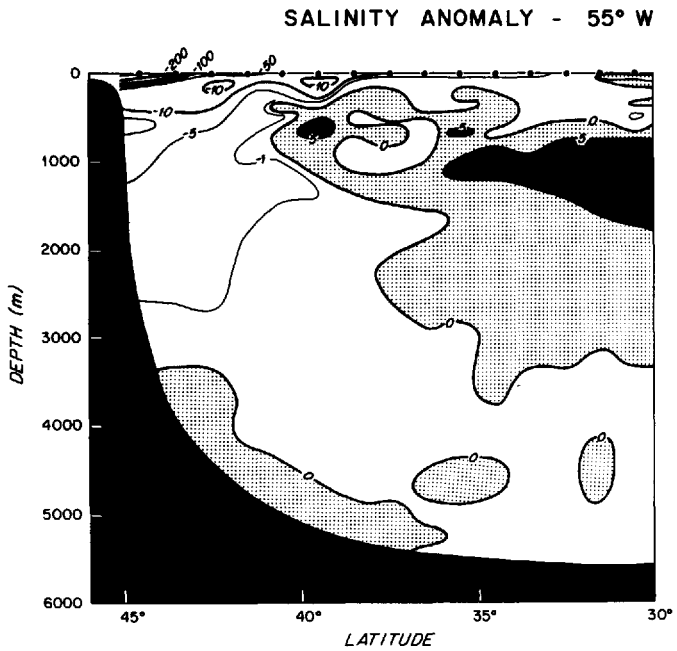

Figure 9c. Section of average salinity anomaly (0.01‰) along 55W. Positive anomalies are shaded. South of 40N and above 1000 m the −1 contour is complicated and was not contoured.

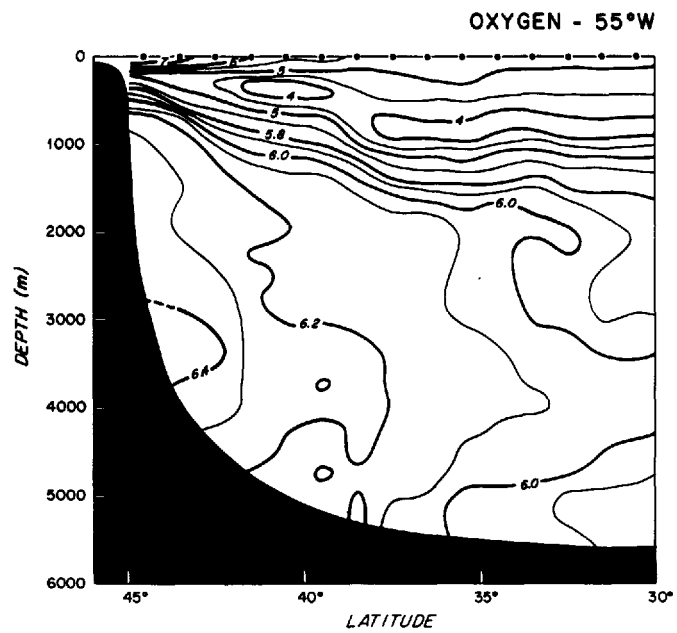

Figure 9d. Section of average oxygen (ml/l) along 55W.

This low salinity water consists of (1) Subarctic Intermediate Water above 500 m and in the general temperature range 5 to 10C and (2) Labrador Sea Water at approximate depths of 500 to 2500 m and temperatures of 3 to 4C. Worthington (1976) has mapped salinity on the 3.4 and 6.0C potential temperature surfaces and showed the southwestward spread of low salinity water bordering the continental slope. Extremely large salinity variations are observed on the 6C surface (Fig. 9c) from +0.1‰ in the Mediterranean Water down to −2.0‰ at the surface near 45N.

Oxygen

A region of high oxygen values >6.3 ml/l hugs the continental slope and rise in depths from 900 to 4300 m and extends 300 km offshore (Fig. 9d). Within this region are two distinct oxygen maxima. The shallowest has a maximum value of 6.40 ml/l and occurs near 2200 m and a potential temperature of 3.6C. The second has a maximum of 6.56 ml/l and lies near 3500 and a potential temperature of 2.2C. The upper maximum is an indication of Labrador Sea Water, the lower of Norwegian Sea Overflow Water. Both water masses flow westward as the Western Boundary Undercurrent. It is noteworthy that the region of westward velocity in the northern countercurrent (Fig. 3a) coincides closely with the region of high oxygen >6.2 ml/l. Southward extensions of the two oxygen maxima are seen as southward pointing wedge-shaped areas which follow the 2.2C and 3.6C isotherms to at least 30N (Fig. 9d).

REFERENCES

Barrett, J. R., Jr. 1965. Subsurface currents off Cape Hatteras. Deep-Sea Res., *12*, 173–184.

Barrett, J. R., Jr. and W. J. Schmitz, Jr. 1971. Transport float measurements and hydrographic station data from three sections across the Gulf Stream near 67W. Woods Hole Oceanographic Institution Technical Report No 71-66.

Bunker, A. F. and R. A. Goldsmith. 1979. Archived time-series of Atlantic Ocean meteorological variables and surface fluxes. Woods Hole Oceanographic Institution Technical Report, WHOI-79-3.

Clarke, R. A., H. W. Hill, R. F. Reiniger and B. A. Warren. 1980. Current system south and east of the Grand Banks of Newfoundland. J. Phys. Oceanogr., *10*, 25–65.

Clarke, R. A. and R. F. Reiniger. 1973. The Gulf Stream at 49°30'W. Deep-Sea Res., *20*, 627–641.

Emery, W. J. 1983. On the geographical variability of the upper level mean and eddy fields in the North Atlantic and North Pacific. J. Phys. Oceanogr. *13*, 269–291.

Fuglister, F. C. 1963. Gulf Stream '60. Progress in Oceanography, *1*, 265–383.

Halkin, D. M. and H. T. Rossby. 1984. The variability of the Gulf Stream at 73W. EOS, *65*, 225, (abstract).

Hogg, N. G. 1983. A note on the deep circulation in the western North Atlantic, its nature and causes. Deep-Sea Res., *30*, 945–961.

Holland, W., D. E. Harrison and A. Semtner. 1983. Eddy-resolving numerical models of large-scale ocean circulation, *in* Eddies in Marine Science, A. R. Robinson, ed., Springer-Verlag, NY, 379–403.

Iselin, C. O'D. 1936. A study of the circulation of the western North Atlantic. Papers in Phys. Oceanogr. and Meteor., *4*, 101 pp.

Knauss, J. A. 1969. A note on the transport of the Gulf Stream. Deep-Sea Res., *16,* (Suppl.), 117–123.

Luyten, J. R. 1977. Scales of motion in the deep Gulf Stream and across the Continental Rise. J. Mar. Res., *35,* 49–74.

McCartney, M. S., L. V. Worthington and M. E. Raymer. 1980. Anomalous water mass distributions at 55W in the North Atlantic in 1977. J. Mar. Res., *38,* 147–172.

McNally, G. J. 1981. Satellite tracked drift buoy observations of the near surface flow in the eastern mid-latitude North Pacific. J. Geophys. Res., *86,* 8022–8030.

Niiler, P. P. and W. S. Richardson. 1973. Seasonal variability of the Florida Current. J. Mar. Res., *31,* 144–167.

Owens, W. B. 1984. A synoptic and statistical description of the Gulf Stream and subtropical gyre using SOFAR floats. J. Phys. Oceanogr., *14,* 104–113.

Owens, W. B. and N. G. Hogg. 1980. Oceanic observations of stratified Taylor columns near a bump. Deep-Sea Res., *27,* 1029–1045.

Richardson, P. L. 1977. On the crossover between the Gulf Stream and the Western Boundary Undercurrent. Deep-Sea Res., *24,* 139–159.

—— 1981. Gulf Stream trajectories measured with free-drifting buoys. J. Phys. Oceanogr., *11,* 999–1010.

—— 1983a. A vertical section of eddy kinetic energy through the Gulf Stream system. J. Geophys. Res., *88*(C4), 2705–2709.

—— 1983b. Eddy kinetic energy in the North Atlantic from surface drifters. J. Geophys. Res., *88*(C7), 4355–4367.

Richardson, P. L. and J. A. Knauss. 1971. Gulf Stream and Western Boundary Undercurrent observations at Cape Hatteras. Deep-Sea Res., *18,* 1089–1109.

Richardson, P. L., J. F. Price, W. B. Owens, W. J. Schmitz, H. T. Rossby, A. M. Bradley, J. R. Valdes and D. C. Webb. 1981. North Atlantic subtropical gyre: SOFAR floats tracked by moored listening stations. Science, *213,* 435–437.

Richardson, W. S., W. J. Schmitz, Jr. and P. P. Niiler. 1969. The velocity structure of the Florida Current from the Straits of Florida to Cape Fear. Deep-Sea Res., *16* (Suppl.), 225–231.

Robinson, A. R., J. R. Luyten and F. C. Fuglister. 1974. Transient Gulf Stream meandering. Part I: An observational experiment. J. Phys. Oceanogr., *4,* 237–255.

Robinson, M. K., R. A. Bauer and E. H. Schroeder. 1979. Atlas of North Atlantic-Indian Ocean Monthly Mean Temperatures and Mean Salinities of the Surface Layer. NOORP-18 Naval Oceanographic Office, NSTL Station, Bay St. Louis, MS, 213 pp.

Schmitz, W. J., Jr. 1977. On the deep general circulation in the Western North Atlantic. J. Mar. Res., *35,* 21–28.

—— 1978. Observations of the vertical structure of low-frequency fluctuations in the western North Atlantic. J. Mar. Res., *36,* 295–310.

—— 1980. Weakly depth-dependent segments of the North Atlantic circulation. J. Mar. Res., *38,* 111–133.

Schmitz, W. J., Jr. and W. R. Holland. 1982. A preliminary comparison of selected numerical eddy-resolving general circulation experiments with observations. J. Mar. Res., *40,* 75–117.

Schmitz, W. J., Jr. and M. S. McCartney. 1982. An example of long-term variability for subsurface current and hydrographic patterns in the western North Atlantic. J. Mar. Res., (Suppl.), *40,* 707–726.

Shaw, P. and H. T. Rossby. 1984. Towards a Lagrangian description of the Gulf Stream. J. Phys. Oceanogr., *14,* 528–540.

Spain, D. L., R. M. O'Gara and H. T. Rossby. 1980. SOFAR float data report of the POLYMODE Local Dynamics Experiment. University of Rhode Island Technical Report, Ref. No. 80-1, 200 pp.

Swallow, J. C. and L. V. Worthington. 1961. An observation of a deep countercurrent in the western North Atlantic. Deep-Sea Res., *8*, 1–19.

Warren, B. A. and G. H. Volkmann. 1968. Measurement of volume transport of the Gulf Stream south of New England. J. Mar. Res., *26*, 110–126.

Worthington, L. V. 1976. On the North Atlantic Circulation. The Johns Hopkins Oceanographic Studies, *6*, 110 pp.

Worthington, L. V. and M. G. Metcalf. 1961. The relationship between potential temperature and salinity in deep Atlantic water. Rapports et Proces-Verbaux des Reunions, Conseil Permanent International pour l'Exploration de la Mer, *149*, 122–128.

Worthington, L. V. and W. R. Wright. 1970. North Atlantic Ocean Atlas. Woods Hole Oceanographic Institution Atlas Series, No. *3*, 190 pp.

Wright, W. R. and L. V. Worthington. 1970. The water masses of the North Atlantic Ocean: a volumetric census of temperature and salinity. American Geological Society Serial Atlas of Marine Environment, Folio No. *19*.

Wunsch, C. 1978. The general circulation of the North Atlantic west of 50W determined from inverse methods. Rev. Geophys. and Space Phys., *16*, 583–620.

Wyrtki, K., L. Magaard and J. Hager. 1976. Eddy energy in the oceans. J. Geophys. Res., *81*, 2641–2646.

Received: *12 March, 1984;* revised: *5 October, 1984.*